Naturally Hydrophobic Foams from Lignocellulosic Fibers Prepared by Oven-Drying

Elisa S. Ferreira, Emily D. Cranston,* and Camila A. Rezende*

Cite This: *ACS Sustainable Chem. Eng.* 2020, 8, 8267−8278

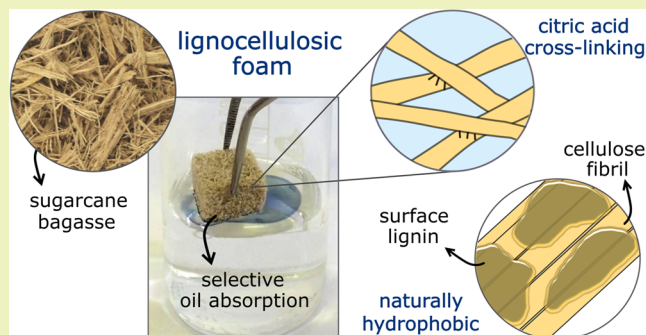Read Online

ACCESS | 📊 Metrics & More | 📰 Article Recommendations | 🆂�🅸 Supporting Information

ABSTRACT: Lignocellulosic sugarcane biomass underwent an alkaline treatment for partial lignin extraction and then foams with very low apparent density (0.09 g/cm^3) were easily obtained by oven-drying aqueous dispersions of fibers. The fiber networks were covalently reinforced through cross-linking by heating the dried material in the presence of citric acid. The lignocellulosic foams were naturally hydrophobic (water contact angle = 117°), without requiring any further chemical modification. The hydrophobicity is attributed to the combination of (1) residual lignin, (2) redeposited lignin that has undergone thermal treatment, (3) the fiber and foam surface roughness, and (4) the structure's ability to trap air. The cross-linked fiber networks showed shape-recovery properties under compressive stress, high absorption capacity, and mechanical resistance when immersed in water and oil. This work demonstrates that lignocellulosic foams from sugarcane bagasse, processed following low cost and green methods, are promising for selective removal of hydrophobic compounds in aqueous environments and in a range of insulating and packaging products.

KEYWORDS: *foam, lignocellulosic fiber, sugarcane bagasse, hydrophobic, lightweight material*

INTRODUCTION

Cellulose foams are porous lightweight materials that can be obtained by drying liquid foams containing cellulosic fibers (with fiber diameters in the range of 15−50 μm).[1] They are usually prepared by the so-called foam-forming method, which consists of incorporating air into an aqueous dispersion of fibers and surfactants followed by oven-drying the liquid foam to obtain a lightweight network with apparent densities as low as 0.005 g/cm^3.[1,2] Recently, we introduced an alternative method to fabricate lightweight cellulosic structures by demonstrating that dispersions of partially hydrolyzed fibers can be dried in an oven without the need for surfactants or air incorporation.[3] This method produces cellulosic matrices free of additives with a network connected by fiber entanglements.

Generally, foams of cellulose fibers can be obtained using scalable processes to remove the solvent,[4] without requiring special drying techniques, such as freeze-drying or supercritical drying. However, these more expensive and time-consuming drying methods are normally needed to produce cellulose aerogels with extremely low density networks, with 0.0002 g/cm^3 being the lowest density reported to date.[5] Such aerogels are often produced by solvent removal from nanocellulose gels (sometimes with cryo-templating prior to drying), as reviewed previously.[6−8] Lightweight materials containing fibers have been investigated for applications in construction, membranes, and packaging since their properties include, for example, high

sound absorption,[2,9] fluid permeability suitable for aerosol filters,[10] and resistance to compressive stress.[3,11]

Under mechanical stress, porous cellulosic materials, such as foams and paper, usually fail when fibers are displaced, due to separation of the network contact points.[10,12] Therefore, the most effective strategy to improve mechanical performance is to reinforce the contact points using chemical cross-linking between two fibers. Networks can be reinforced based on resins (amine-epichlorohydrin, urea-formaldehyde, melamine-formaldehyde, and glyoxalated polyacrylamide), oxidized polysaccharides (aldehyde-modified starch or cellulose), and polycarboxylic acids (citric, succinic, and maleic acid), which are chemicals widely used as paper wet-strength agents.[13] Similarly, (nano)cellulose aerogels and foams can be reinforced by linking cellulose hydroxyl groups with polymers and resins, by ionically cross-linking anionic charge groups on the cellulose surface or by bringing functionalized surfaces (e.g., hydrazide and aldehyde-modified cellulose) into contact.[8,14] Citric acid is a green cross-linker used as a strength additive[13]

for paper and gel promoters for cellulose derivatives;[15−17] however, it has not been extensively explored in other cellulosic materials. The few examples that exist in the literature include using citric acid to cross-link bacterial cellulose networks,[18] lightweight materials of cellulosic fibers with chitosan,[19] and conductive devices produced from phosphorylated cellulose.[20]

Compatibility between cellulose and polymers, or cellulose and nonpolar solvents, can be improved by modifying the cellulose surface chemistry following a large range of well-known carbohydrate chemistries. Cellulose is a biopolymer of glucose with a high density of hydroxyl groups that form strong hydrogen bonds with water,[21] and although the cellulose crystalline structure is sometimes considered amphiphilic,[22] for practical wettability purposes, surface modification is required to make cellulose truly hydrophobic.[23] Strategies to favor cellulose interactions with hydrophobic compounds are particularly needed in applications such as plastic composites, emulsions, and oil recovery, or where water absorption would be highly detrimental.[24−26]

There are several approaches to hydrophobize cellulose surfaces, such as esterification,[27] acetylation,[28] polymer grafting,[26] wax coating,[29] the use of tannic acid coupled with alkylamines,[30] etc.[31] In nature, wettability of cellulosics is altered by lignin,[32,33] but this effect has not been fully exploited in materials engineering and some of the fundamentals are still under investigation. Only a few works explore using lignin as a hydrophobizing agent for cellulose, for example, Rojas and co-workers evaluated the impact of residual lignin on nano-papers[34] and papers,[35] preparing surfaces with water contact angles up to 82°, which are more hydrophobic than the pure cellulosic substrates. Similarly, micro/nanocelluloses with residual lignin are claimed to be more hydrophobic,[36] and recently, the incorporation of lignin has also been used in regenerated cellulose hydrogels to alter the pore structure and increase the chemisorption of metallic cations.[37]

In this work, sugarcane bagasse was chosen as a lignocellulosic feedstock to produce lightweight foam materials. Global sugarcane production exceeds one billion tons per year, and bagasse is the waste obtained after sugarcane processing, representing 30% of the pristine biomass.[38] Significant efforts have been made to fractionate bagasse components for conversion into fuels, materials, and chemicals to gain value from this plentiful agricultural waste.[39,40] Here, we propose a green strategy to prepare naturally hydrophobic foams using cellulose fibers from sugarcane bagasse that contains a portion of their native lignin. Partial extraction of lignin was employed as a pretreatment to make cellulose more accessible for cross-linking and roughen the fiber surfaces. Citric acid was added to pretreated fiber dispersions as a heat-activated cross-linker of cellulose followed by oven-drying to produce lightweight, porous, and wet-resilient materials.

■ EXPERIMENTAL SECTION

Materials. Sugarcane bagasse was kindly donated by Cosan Group (Ibaté, Brazil). Citric acid (≥99.5% purity) and corn oil were purchased from Sigma Aldrich and NaOH (>97.0% purity) from Caledon. All water used was Millipore Milli-Q grade distilled deionized water (DIW, 18.2 MΩ.cm resistivity), and unless otherwise noted, all measurement values reported/plotted are averages with their associated standard deviation.

Bagasse Pretreatment. Sugarcane bagasse was milled using a blender (Magic Bullet MB1001C, SGS) until particles could pass through a 425 μm mesh sieve (Canadian Standard Sieve Series n 40,

W. S. Tyler Company of Canada). Lignin was partially extracted from milled fibers using a pretreatment with 2% w/v NaOH at 120 °C for 1 h in an aging cell (UNS S30300 Type 303, Ofite), as described previously.[41] After extraction, fibers were collected using a 125 μm mesh sieve (Canadian Standard Sieve Series n 120, W. S. Tyler Company of Canada) and were rinsed with deionized water until neutral pH.

Foam Preparation. Pretreated fibers were dispersed at 40 g/L in an aqueous solution of citric acid (1.4 g of citric acid to 1 g of fibers). In sequence, 20 g of the dispersion was placed in a cylindrical mold of stainless steel (30 mm height, 26 mm diameter) with a permeable mesh bottom. Dispersions were dried at 60 °C in a convection oven (Symphony, VWR) until constant weight, and after that, a thermal treatment at 150 °C for 5 min was used to promote citric acid cross-linking.[18,19] The cross-linked foams were rinsed with water to remove the excess citric acid not covalently linked to the fibers, until the conductivity of the rinsing water was equal to that of deionized water. After rinsing, cross-linked materials were dried in an oven at 60 °C. The 1.4:1 weight ratio of citric acid to fibers was based on a previous report using citric acid to pretreat lignocellulosic fibers.[42] Usually, protocols to cross-link cellulosic fibers require a huge excess of acid (1.7:1 weight).[19] We attempted to reduce the amount of citric acid needed but found that cross-linking was insufficient to hold the foams together in water. Because rinsing easily removed the large excess of citric acid and the cost and environmental impact of this reagent is low, we do not see this as a significant barrier to scale-up. For comparison, foams without cross-linking were also prepared by dispersing pretreated fibers in water (without citric acid), following the same foam preparation protocol.

Lignin Precipitation Tests. Foams containing "extra" lignin were prepared by incorporating the lignin that was extracted during the alkaline pretreatment (0.8% w/v lignin dissolved in 2% w/v NaOH aqueous solution). Pretreated bagasse fibers were dispersed at 40 g/L in the liquid phase that remained after the alkaline treatment followed by heating at 120 °C for 30 min in an aging cell (UNS S30300 Type 303, Ofite). After the thermal treatment, fibers were collected using a 125 μm mesh sieve and were rinsed with deionized water until neutral pH. The fibers with "extra" lignin were dispersed in water, and foams were prepared in cylindrical molds by drying at 60 °C in a convection oven (Symphony, VWR). For comparison, foams were prepared from the dispersion of pretreated fibers with "extra" lignin, without thermal treatment, by drying at room temperature. Excess lignin and NaOH were removed by rinsing the foams with water followed by drying at 60 °C in a convection oven.

Fiber Quality Analyzer (FQA). Fiber morphological parameters were acquired in a high resolution FQA (LDA02, OpTest Equipment), equipped with a polarizer and a CCD camera. Briefly, fibers were dispersed in water at approximately 0.02% w/v, and measurements were conducted in flux. Three dispersions were prepared and measured for each sample.

Mechanical Testing. Foams were cut into a cubic shape and compressed at 1.3 mm/min, according to the ASTM D695 standard. Compressive testing was carried out under dry conditions and with samples immersed in water or in corn oil, using a universal testing machine (model 3366, Instron). For shape-recovery measurements, samples were compressed to 40%, then the load was released, and the size recovered by the specimen was immediately measured with a caliper. Sample sizes after releasing the compressive load were also determined after 4 h with the specimen immersed in water, and after it was allowed to dry under ambient conditions. At least six specimens per sample were used in each test.

Fourier-Transform Infrared Spectroscopy (FTIR). Infrared spectra of foams were collected using attenuated total reflectance (ATR) mode in a spectrometer (Nicolet 6700, Thermo Scientific) operating at 64 scans and 0.482 cm⁻¹ steps.

Stability in Water. Foams with and without cross-linking were placed in a beaker of water where they were observed to float on the water surface for several hours. To promote wetting, the foams were pushed into the water phase with a glass rod and they were vigorously

stirred with a magnetic stir bar for 15 s to evaluate their stability in water.

Oil Absorption Measurements. Foams were immersed in corn oil overnight under ambient conditions and oil absorption capacity was determined by gravimetry. Visually, oil absorption occurred instantly when the foams were in contact with oil, but the immersion time was long to ensure equilibrium absorption, excluding any kinetic effect due to oil viscosity. Samples with and without cross-linking were measured in duplicate.

Lignin Content. The lignin fraction in fibers before and after the alkaline pretreatment was determined based on the acetyl bromide-soluble lignin method.[43] Briefly, 4 mg of fibers were added to a 25% acetyl bromide solution and kept at 50 °C for 3 h. After the reaction, 1 mL of 2 mol/L aqueous NaOH and 175 μL of 0.5 mol/L hydroxylamine in HCl solution were added. Solutions were diluted in pure acetic acid, and their absorption at 280 nm was determined using a UV/VIS diode array spectrophotometer (model 8453, Agilent Technologies).

Field-Emission Scanning Electron Microscopy (FESEM). Electron micrographs were acquired in a FESEM Quanta 650 microscope (FEI), operating at a 5 kV accelerating voltage and using a secondary electron detector. For microscopy analysis, bagasse fibers were fixed on a stub with copper tape and coated with gold using a SCD 005 coater (Bal-Tec) equipped with a planetary drive stage.

Apparent Density and Porosity Determination. Samples were cut in a cubic shape (25 mm × 25 mm) using a table saw and their volume was calculated from the dimensions determined using a caliper. Compared to nanocellulose aerogels, these lignocellulose foams were easily cut to the desired dimensions. Apparent density (ρ_{app}) is the ratio between the mass and the total volume of the foam, including fibers and voids. The density of pretreated bagasse fibers (ρ_{fiber}) was calculated according to the fiber composition (% by weight of each component) and the density of each component ($\rho_{cellulose} = 1.59$; $\rho_{hemicellulose} = 1.52$; $\rho_{lignin} = 1.45$ g/cm^3).[44,45] Finally, foam porosity (P_{foam}) was estimated using eq 1.

$$P_{foam} = \left(1 - \frac{\rho_{app}}{\rho_{fiber}}\right) \times 100 \tag{1}$$

X-ray Computed Microtomography (Micro-CT). Bagasse foams were scanned as-prepared, without staining, in a 3D X-ray microscope (Skyscan 1272, Bruker), operating at 20 kV and 175 μA, with a 0.4° rotation step, recording two frames per position, at a 21.6 μm resolution (1224 × 1224 pixels). Structures were reconstructed on NRecon software (SkyScan), applying ring artifact correction number 20 and smoothing correction level 1, for noise reduction. For reconstruction, contrast limits of the electronic density were set in the same range for each sample, allowing comparisons. DataViewer software (SkyScan) was used for visualization and image acquisition.

Contact Angle Measurements. Static contact angle measurements between a water droplet and the foam surface were acquired in a Drop Shape Analyzer (DSA100, Krüss). Droplets of 2 μL were deposited on the surface, and measurements were performed every 10 s for 1 min, using Krüss ADVANCE software. The contact angle was constant over this time period, and measurements were taken at three different locations on the sample surface.

Atomic Force Microscopy with In Situ Infrared Spectroscopy (AFM-IR). Bagasse fibers pretreated with 2% NaOH were analyzed using an atomic force microscope (NanoIR2-s, Anasys). Prior to analysis, fibers were fixed on a metallic substrate with a thin layer of epoxy adhesive. Scanning was carried out using a tip coated with gold with a radius of approximately 30 nm (contGB, Buget Sensors). The probe was placed on a site of interest chosen in an AFM map, and spectra were acquired illuminating the sample with an IR laser (1550−1800 cm^{-1}), in contact mode, as described elsewhere.[46] The thermal expansion of that site caused by IR absorption was monitored by the response in the resonance vibration of tip cantilever. Analysis Studio software (Anasys) was used for visualization and image acquisition.

■ RESULTS AND DISCUSSION

Partial Delignification of Sugarcane Bagasse. Sugarcane bagasse is an abundant agricultural waste, obtained after crushing and extracting the juice from sugarcane culm for sugar and ethanol production. This residue comprises the ground vascular bundles and sucrose-storage parenchyma cells that were present in the sugarcane culm.[47] Bagasse is therefore mainly composed of plant cell walls, i.e., a composite of cellulose, lignin, and hemicellulose.[41]

Lignin is a polyphenol that, when treated with alkaline solution, is fragmented due to the breaking of ether-aryl and diphenyl ether linkages. In alkaline pH, these fragments can be extracted to the aqueous phase by deprotonation of lignin-derived phenolic structures.[48] The *in natura* sugarcane bagasse (untreated) had 25 wt % lignin and, after undergoing our mild alkaline pretreatment (2% NaOH at 120 °C for 1 h), the lignin content was decreased to 17 wt %, representing a substantial extraction of the lignin (Supporting Information, Table S1). Importantly, this component extraction and the fiber swelling during the pretreatment caused disruption of the plant cell wall structure and significant morphological changes, which were apparent by FESEM (Figure 1) and agree with the previously demonstrated fiber morphologies.[41]

The *in natura* bagasse fibers appear as parallel fibers, which are the vascular bundles from sugarcane culm, covered by residual parenchyma cells (Figure 1a). These cells are rounded vacuoles in the plant,[49] but in the FESEM micrographs they appear as flat structures on top of the fibers due to the crushing and drying processes that cause collapse. After the 2% NaOH pretreatment, the parenchyma layer appeared to be partially removed, exposing the vascular bundles, as shown by the parallel tube assemblies (Figure 1b,c). Cohesion in the plant cell wall is usually attributed to the presence of lignin,[50−52] which supports that the pretreated fibers with less lignin are partially fibrillated.

Changes in the fiber format can be further quantified according to geometric features such as fiber width and fiber kinks, which are sharp bends resulting from where fibers are deformed during refining and mechanical treatment.[53] After alkaline pretreatment, the fiber kink index increased from 1.82 ± 0.06 to 2.20 ± 0.04 kinks per mm (Figure 1d), indicating that fibers had a higher number of kinks and/or higher curvature angles in these bends, compared to bagasse *in natura*. These values imply that the fibers have been softened, or made more flexible, from the pretreatment that removed some of the lignin "glue". The kink index values measured here are generally within the range of those reported previously for bagasse fibers (1.89 kinks per mm)[54] and are higher than the values found for stiffer wood pulp fibers destined for paper products (0.4−0.6 kinks per mm).[55] The fiber widths measured by an FQA also decreased from 33.4 ± 0.6 to 31.3 ± 0.1 μm after pretreatment, further indicating that significant removal of some surface material has occurred. This reduction in the fiber diameter was also evident by FESEM (Figure 1a−c).

The inferred structural organization of sugarcane culm through the various processing steps to the pretreated bagasse used herein to produce foams is summarized in Figure 2: Figure 2a shows the vascular bundles aligned in the longitudinal direction for sugar, water, and nutrient transport (fiber diameter of 20−60 μm) and the bundles are surrounded by parenchyma cells organized in a honeycomb-like structure
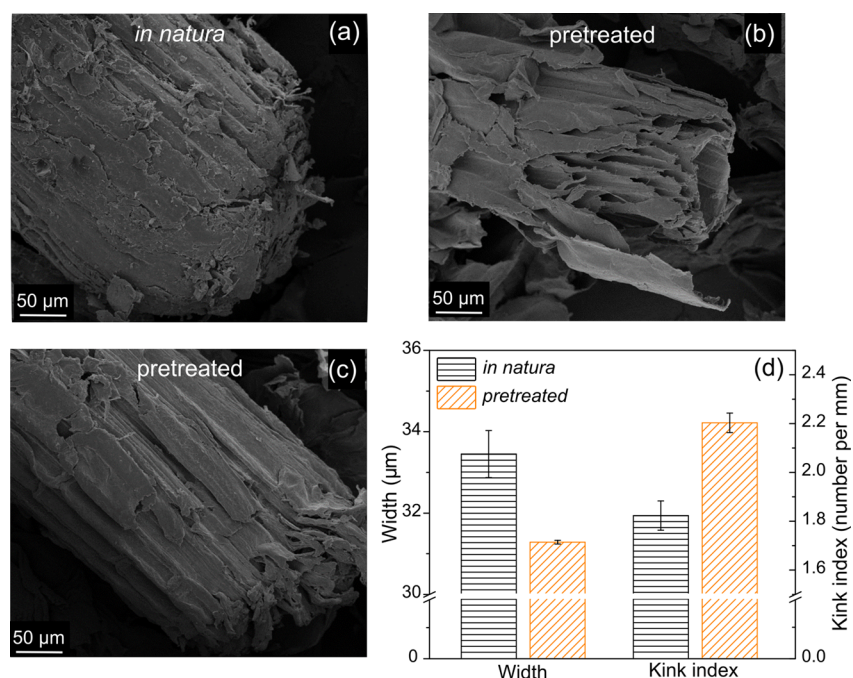
Figure 1. Morphological comparison between sugarcane bagasse samples; FESEM micrographs: (a) *in natura*; (b−c) fibers after pretreatment with 2% NaOH (to show variability between fibers treated identically); and (d) fiber width and kink index determined by FQA.
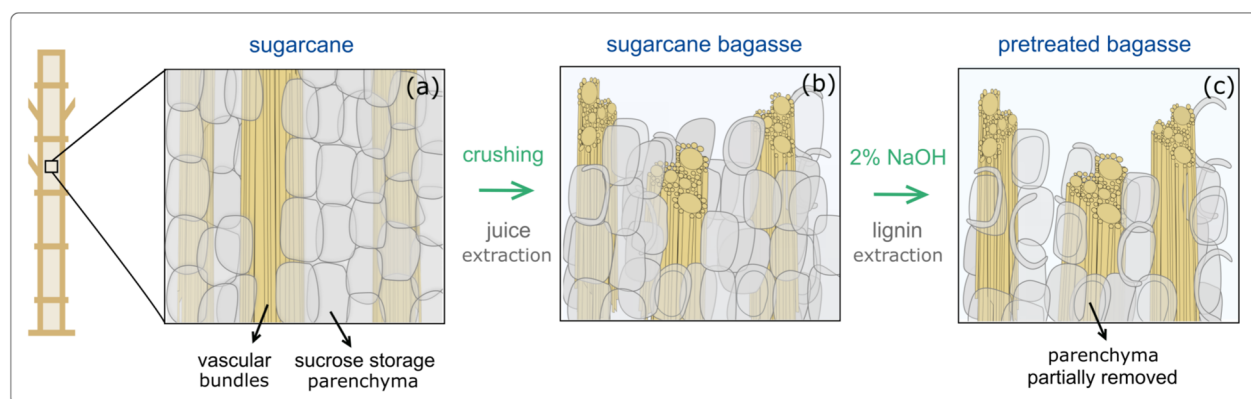

Figure 2. Schematic representation of the structural architecture of sugarcane: (a) sugarcane culm; (b) *in natura* sugarcane bagasse, obtained after crushing sugarcane culms; and (c) sugarcane bagasse after alkaline pretreatment.

(cell diameter of 50−200 μm).[56] Figure 2b shows that when sugarcane culms are milled, parenchyma cells are disrupted (which releases the sucrose-rich juice) but some parenchyma tissue still remains in the sugarcane bagasse with intact or damaged cells.[57] Finally, after the NaOH pretreatment, Figure 2c shows a partial removal of residual parenchyma cells, which are structures with lower lignin content than the inner vascular bundles.[58] Overall, the fibers become rougher without the parenchyma coating and both cellulose-rich regions (where lignin is extracted) and lignin-rich components (vascular bundles) are exposed.

Structure of the Lignocellulosic Foams. After partial lignin extraction, the aqueous dispersions of pretreated bagasse fibers were oven-dried to give uniform lightweight foams. Foams with and without citric acid cross-linking were prepared and were indistinguishable in the dry form (Figure 3a,d). When the foams were placed in water, initially those with and without cross-linking floated on the water surface (Figure 3b,e) but, after vigorous magnetic stirring for 15 s, only the cross-

linked foam maintained its structure (Figure 3c,f). This is attributed to the covalent reinforcement that occurred when fibers were oven-dried in the presence of citric acid, which are conditions that favor cellulose esterification with citric anhydride (Figure 3g).[13] The FTIR spectrum of the (extensively rinsed) cross-linked foam was acquired by a surface sensitive technique (ATR with penetration depth < 1 μm) and indicated that citric acid had successfully reacted with the fiber's exposed cellulose, showing a band at 1740 cm^{-1}, which corresponds to the carbonyl stretch (Figure 3h). This band was not observed in the samples prepared using fibers pretreated with 2% NaOH but not cross-linked (orange curve in Figure 3h).

The foam reinforced with citric acid had an apparent density of 0.096 ± 0.001 g/cm^3, equivalent to the non cross-linked foam (0.092 ± 0.003 g/cm^3) (Figure 3i), suggesting that cross-linking did not alter the internal structure or cause significant material shrinkage. These values are close to the densities of lightweight packaging materials (e.g., corrugated paperboard,
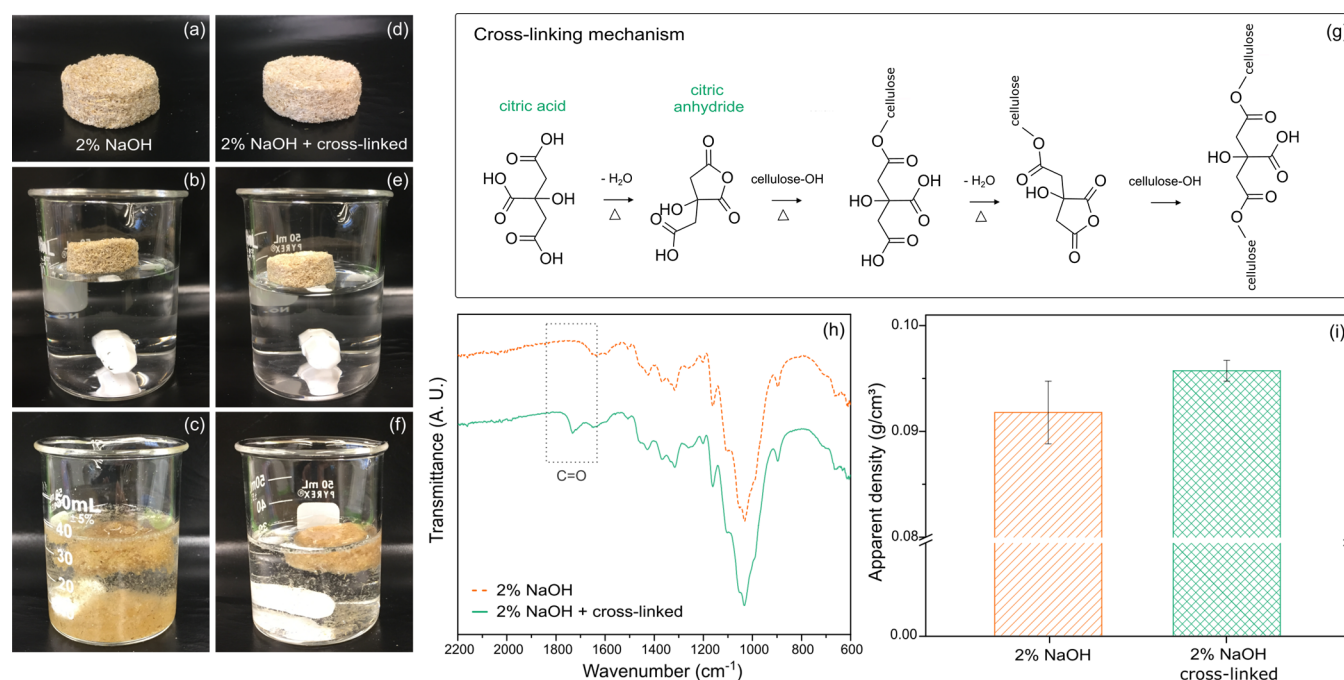
Figure 3. Lignocellulosic foams prepared from sugarcane bagasse pretreated with 2% NaOH: (a−c) without and (d−f) with cross-linking; (a, d) as-prepared; (b, e) on the water surface; (c, f) after vigorous magnetic stirring for 15 s; (g) mechanism for cross-linking between cellulose molecules by citric acid, based on the work by Demitri et al.;[15] (h) ATR-FTIR spectra of foams prepared from pretreated fibers with (green) or without (orange) citric acid cross-linking, showing changes in the carbonyl region at 1740 cm^{-1}; and (i) apparent density of foams prepared without (orange, line pattern) and with chemical cross-linking (green, cross-hatch pattern).

0.03 g/cm^3)[59] and lower than those of efficient absorbent materials (e.g., blotting paper, 0.4 g/cm^3).[60] Our previously reported foams prepared from eucalyptus pulp, also made by oven-drying but with a different pretreatment (i.e., H$_2$SO$_4$), are denser (0.15 g/cm^3).[3] However, when cellulose fibers are mixed with surfactants and air is incorporated, density values as low as 0.005 g/cm^3 can be achieved[1] (for basis weight comparison and calculations, see Supporting Information, Table S2). For applications in protective packaging or as absorbent materials, network structure and mechanical properties must also be considered alongside density, and as such, these parameters are discussed next.

X-ray computed microtomography images were acquired for cylindrical foam samples to analyze the internal structure of their fiber network (Figure 4). Morphological analysis showed similar networks with and without cross-linking, again indicating that the fiber assembly was not affected by citric acid reinforcement. This supports that the main role of citric acid was to produce materials with strong fiber−fiber bonds that did not redisperse in liquid. The foam network consisted of fibers arranged in an open cell wall configuration, forming macropores (for more details, see FESEM cross-sectional analysis and micro-CT video, in the Supporting Information, Figure S1 and Video S1). Micro-CT showed that the fibers were uniformly distributed in the foams, without any discernible concentration gradients, evidencing that the fibers did not settle during the drying process (blue and green planes in Figure 4).

Bright spots in the micro-CT images (Figure 4) were distributed throughout the structure and appear due to higher density portions of the sample. These denser regions could be identified as granular particles in the reconstructed 3D image (Supporting Information, Figure S2 and Video S1), and they are likely silicates from sugarcane, identified as Si by X-ray

photoelectron spectroscopy (XPS) (Supporting Information, Table S3). Similar inorganic components in sugarcane bagasse have been visualized previously using micro-CT.[61]

Mechanical Properties of Lignocellulosic Foams. Mechanical testing revealed that lignocellulosic foams could resist compressive strain without failure, following a mechanical profile that was similar to polymeric foams[62] and cellulose lightweight materials[3] with three regimes: (1) linear, (2) plateau, and (3) densification (Figure 5a). The presence of citric acid cross-linking did not change the stress−strain curve substantially compared to the non cross-linked foam, but it did increase the compressive modulus (in air) from 0.32 ± 0.03 to 0.46 ± 0.07 MPa (Figure 5b), showing that the lignocellulosic network could be successfully reinforced by using a simple and green cross-linking process. If the compressive modulus is normalized by density, the value obtained for cross-linked lignocellulosic foams (ca. 5 MPa cm^3/g) is very similar to the specific modulus reported for cryogels made from pretreated bagasse.[63] This similarity is due to the common building blocks derived from sugarcane bagasse in both materials. When not normalized by density, the compressive modulus reflects a property of the foam structure, as a whole piece. In this case, the mechanical stiffness of our lignocellulosic foams was higher than the one obtained when bagasse was applied to construct cryogels (compressive modulus 0.088 MPa),[63] indicating that our foams were stiffer and needed higher stress to be deformed. The cross-linked foams were also compressed in oil and water and the moduli were calculated (Figure 5b); non cross-linked foams could not be tested in liquid environments because they disintegrated. Interestingly, compression in oil was very similar to compression in air, only compression in water showed a significantly softened material (compressive modulus decreased 30 times to 0.016 MPa). This implies that the interactions between fibers and oil did not alter the
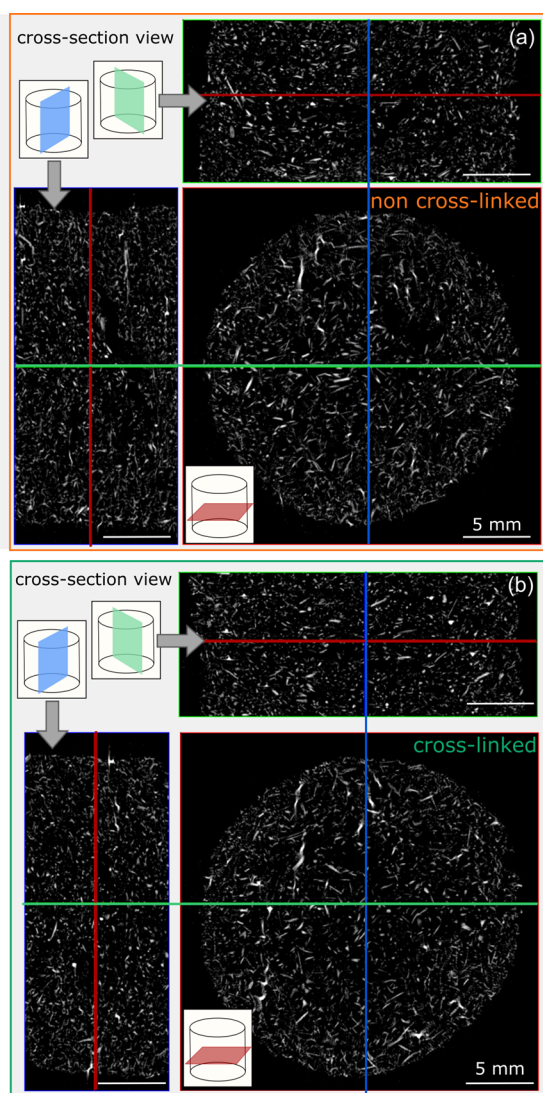
Figure 4. Reconstructed micro-CT images of lignocellulosic foams showing cross-section views from cylindrical samples: (a) non cross-linked; (b) cross-linked.
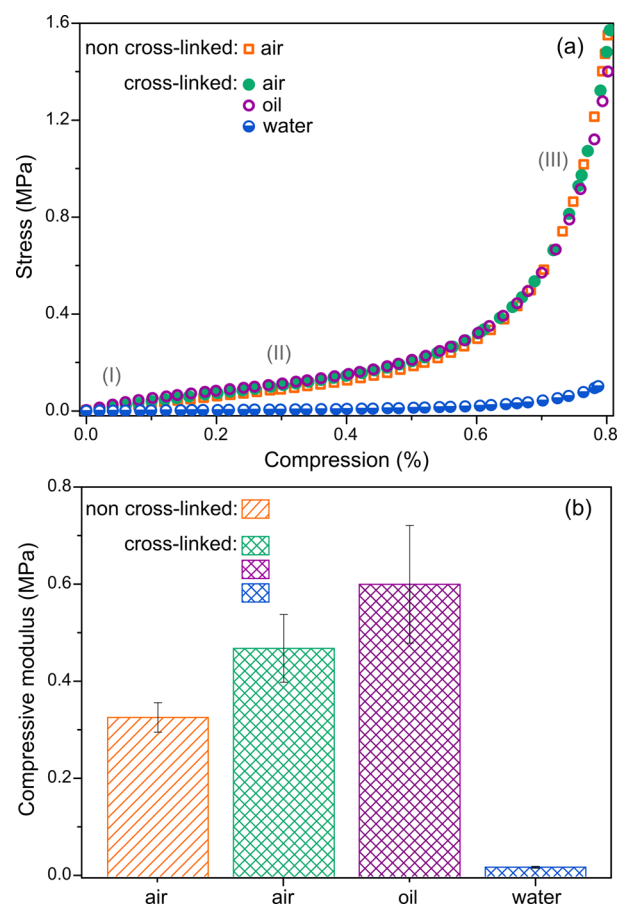

Figure 5. Mechanical testing under compressive strain of lignocellulosic foams without cross-linking in air (orange, line pattern), and cross-linked materials (cross-hatch pattern) in air (green), oil (purple), and water (blue): (a) representative stress–strain diagrams with three compressive regimes (I) elastic, (II) plateau, and (III) densification; (b) compressive modulus taken from the elastic region (<5% strain).

resistance of the fibers nor the strength of the network contact points.

The decrease in modulus for lignocellulosic foams in water is attributed to the plasticizing effects of water and such mechanical fragility is well known for cellulosic fiber materials, such as paper.[64] This effect is generally attributed to water–cellulose hydrogen bonds replacing cellulose–cellulose hydrogen bonds and reducing fiber–fiber interactions.[65] However, Hirn and co-workers used AFM force-distance measurements to show that hydrogen bonding does not contribute significantly to fiber adhesion.[66,67] According to their work, fiber adhesion is more related to the plastic deformation of fibers that takes place during drying.[66,67] As a result, when fibers are rehydrated, swelling affects the fiber dimensions and undoes the contact points between neighboring cellulose chains, which facilitates fiber slippage.[68] Therefore, the most effective strategy to improve mechanical properties of fiber-based materials is to use chemical cross-linking to maintain the contact points between fibers during swelling,[69] as we have done here by heating the foams in the presence of citric acid to induce cross-linking.

The highly elastic behavior of cross-linked foams in water was impressive, implying that they may find application as absorbent materials that could be used to take up liquid followed by compression to empty the pores and then be reused: Figure 6a shows that stress increased linearly up to 40% compression and was reversible. This led to shape-recovery properties, i.e., when the compressive load was released, the foams were restored to 94 ± 1% of their initial height almost immediately, and after 4 h in water, recovered 97 ± 1% (Figure 6b,c). After air-drying the compressed and recovered foams, the final height was still 93 ± 3%, which is an extraordinary result for porous lignocellulosic materials. Typically, cellulosic aerogels and foams collapse due to capillary forces when dried under ambient conditions from the wet state. This supports that the strength of the individual fibers, modulus of the network, and covalent cross-linking between the fibers all work together to produce a novel material that maintains and recovers its structure under a variety of mechanical and environmental conditions. The mechanical response observed here is akin to wet resiliency of paper (when a soaked crumpled paper recovers its planar shape), which is also achieved through extensive fiber cross-linking.[70] These same factors are the reason that the foams can be produced by simple oven-drying without requiring methods
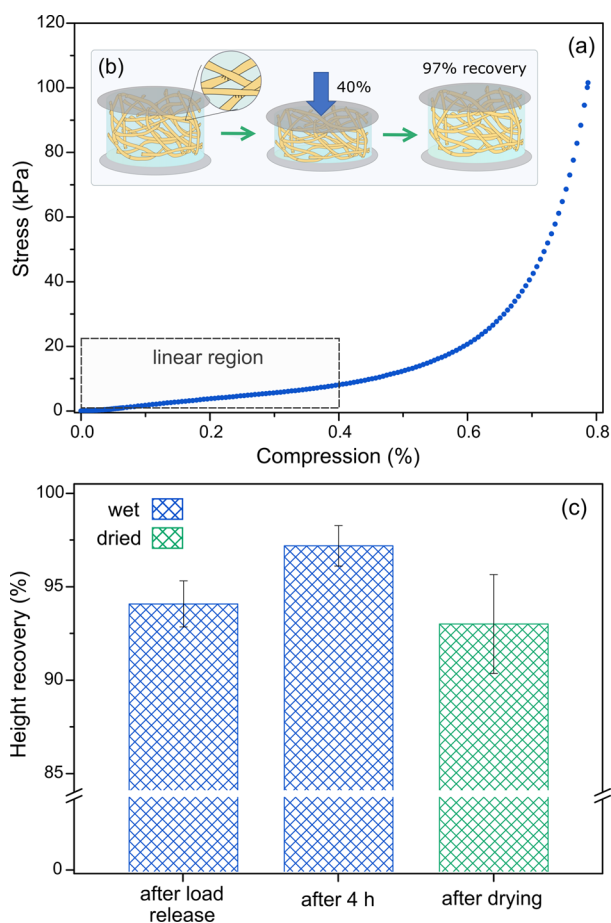
Figure 6. Mechanical testing under compressive strain of cross-linked foams in water: (a) representative stress–strain curve showing the linear region between 0 and 40% compression; (b) schematic representation of the shape-recovery test illustrating a foam being compressed to 40%, and recovering to its original size after load release; (c) percentage of height recovery after compression in the linear region (40% compression) immediately after load release in water (blue); after relaxation in water for 4 h (blue); and after drying (green).

that minimize surface tension, like freeze-drying and critical point drying.

The compression tests also revealed that the network structure in our bagasse foams was capable of storing and dissipating mechanical energy, without significant loss through plastic deformation, which would be beneficial in shock and sound absorbing materials, such as those used in construction, sports gear, and packaging. This effect can be understood using polymeric foams as a model, where the foam cell walls are deformed under compression, occupying empty spaces in the structure (pores), and when the compressive load is released, the cells are restored to their original size.[62] On the other hand, the flexibility and elasticity of our foams are in stark contrast to other high-performance porous materials like silica aerogels, cement foams, and ceramics, which often suffer from brittleness and collapse by brittle crushing when compressed.[62,71] The low fracture toughness of these more conventional porous materials limits the load that such structures can absorb without being crushed; the potential to replace these materials with lignocellulosic foams (and envision entirely new applications) seems promising based on the mechanical properties measured here.

Surface Properties of Lignocellulosic Fibers and Foams.
Fibers and foams that can selectively ad/absorb hydrophobic compounds are desired for applications involving extractions, effluent treatment, and oil spill cleanup.[24−26] For such uses, cellulose surfaces need to be more hydrophobic. Usually, this is achieved through chemical modifications such as esterification[72] or silanization[73] (particularly if super-hydrophobic character is required). Lignin is intrinsically more hydrophobic than cellulose[74] and may be useful in achieving target surface properties. However, the wetting properties of lignin change when it is extracted from the plant cell wall. Redeposited lignin usually tends to increase the hydrophobicity on a cellulosic surface, but the maximum contact angles achieved have been limited to ca. 80°.[34] Similarly, lignin extraction and precipitation in aqueous solution has been shown to produce water-dispersible lignin nanoparticles;[75,76] this compatibility with water indicates that a somewhat hydrophilic character is present in these extracted lignin fragments.

The change in surface energy of extracted lignin can be explained by the fact that the extraction process requires bond cleavage, introducing new functional groups and decreasing molecular weight. For instance, fragmentation by the Kraft method adds thiol groups to the fragments,[77] and the sulfite method causes sulfate group addition,[48] which increases the amount of hydrophilic moieties in the extracted lignin fragments. Moreover, molecular weight reduction may cause conformational changes in lignin fragments as well.[78]

In this work, our strategy was to partially extract the lignin in order to expose the cellulose in the bagasse fibers (vascular bundles)[51,52] for cross-linking, and to keep a part of the lignin in its original chemical and conformational state to assure some hydrophobic character in the final structure. We also recognized that the lignin solubilized at high pH and temperature during alkaline pretreatment may be precipitated and redeposited on the fibers during the rinsing process (that lowers the pH and temperature and thus lignin solubility). Precipitation of lignin was previously observed in sugarcane bagasse samples that were pretreated with NaOH solution[52] and in other fibers that underwent alkaline treatment followed by rinsing with water, such as eucalyptus bark.[51] Lignin redeposition is usually an undesirable effect because it changes fiber wettability, impairing, and the enzymatic performance of cellulases that are used for bioethanol production.[33]

The bagasse foams produced here were highly hydrophobic, as shown by their ability to float on water (Figure 3b,e) and their water contact angle (θ) of 117 ± 8°, with the highest measured value of 127° (Figure 7a). The high θ value for a material mainly composed of cellulose was likely due to the
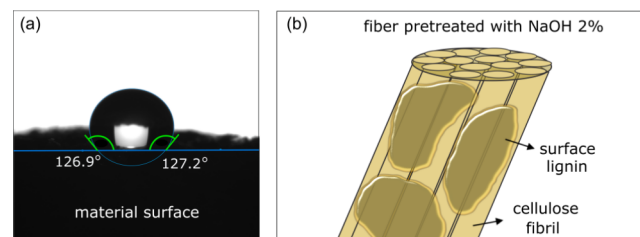

Figure 7. Surface properties of lignocellulosic foams with citric acid cross-linking: (a) water drop on the top of the material with a contact angle of 127°; (b) schematic representation of bagasse fibers pretreated with 2% NaOH, showing lignin domains on its surface.

combination of residual hydrophobic lignin, the increased fiber (nanoscale) roughness from extracted and redeposited lignin (Figure 7b), and the microscale roughness and structure of the foam itself. However, we believe that the redeposited lignin only played a minor role such that when a foam was prepared with fibers that only had residual lignin (achieved by rinsing fibers at the end of the pretreatment step with hot 2% NaOH to prohibit lignin precipitation) the foam wettability was similar to the results shown here. Overall, we observe that if water does not wet the fiber/foam surface then the pores in the foam do not fill with water and the entire structure continues to float (or support a water droplet, depending on the test being performed).

The hierarchical and rough micro/mesostructure of the foam and its ability to trap air are likely the most crucial contributors to hydrophobicity. In fact, the foam is approximately 93% porous (calculated from eq 1) of which these pores are filled with air. Line scans extracted from the micro-CT data at the top of the foam showed surface roughness with heights fluctuating up to 120 μm (Supporting Information, Figure S3). We observed that fibers with identical pretreatment but dried under compression to form a sheet rather than a foam, instantly absorbed water (Supporting Information, Figure S4). This agrees with the theory prescribing that roughened hydrophobic substrates ($\theta > 90°$) have a larger surface area and higher apparent contact angles than for flat surfaces.[79,80] Furthermore, even hydrophilic surfaces can be made hydrophobic/superhydrophobic with the correct geometries, such as mushroom-like microstructures that trap air under the "overhang" and structures with hierarchical micro- and nanoroughness;[79] both of these geometries are possible from our roughened and flattened-fiber containing foams.

The ability for the 2% NaOH pretreatment to produce lignin-rich areas at the fiber surface and increase roughness was investigated by infrared nanospectroscopy. Chemical bonding regions could be probed with a resolution of approximately 30 nm using the AFM-IR technique (Figure 8). The surface of lignocellulosic fibers showed distinct domains of nanoscale roughness that could be identified in topography and deflection images (Figure 8a,b). Line scans from the topography map illustrated a lower roughness region near the line positioned in the top right corner of the image (line 1, Figure 8c), and a higher roughness region in the bottom left (line 2, Figure 8c). IR spectra revealed that the chemical composition of these domains was different (Figure 8d): the region with more uniform contrast (top region, Figure 8b) presented a characteristic carbonyl signal at 1740 cm^{-1} (purple markers and spectra), while the regions with higher roughness (bottom region, Figure 8b) showed no carbonyl peaks (gray markers and spectra). The presence of carbonyl compounds on the surface can arise from both lignin and hemicelluloses present in sugarcane fibers. As lignin is the compound responsible for the hydrophobic character of the foams (hemicelluloses are hydrophilic), domains containing carbonyl bands are primarily attributed to lignin. Additionally, spectra from lignin domains also showed a band assigned to aromatic ring stretch (1618 cm^{-1}), and most of the signals were equivalent to AFM-IR spectra of pure lignin samples (for more details, see Supporting Information, Figure S5). Other superficial regions identified in AFM-IR analysis (gray) were mainly composed of cellulose.
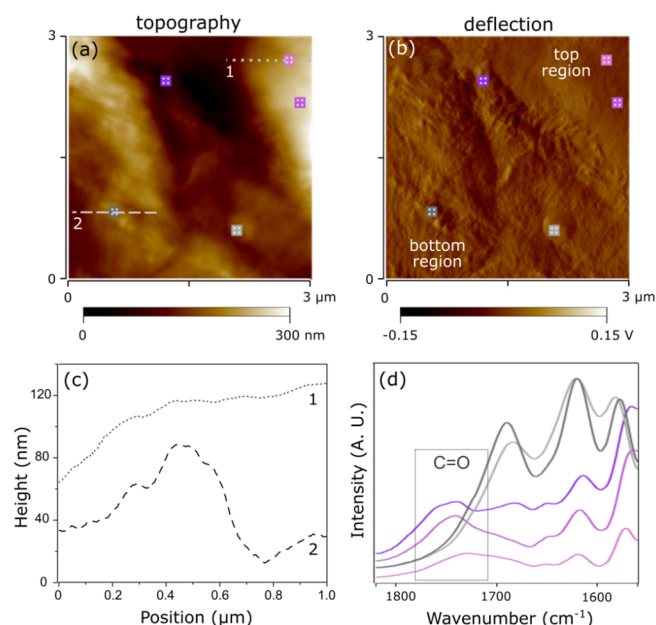

Figure 8. AFM-IR micrographs of sugarcane bagasse fiber surface pretreated with 2% NaOH: (a) topography; (b) cantilever deflection; (c) line scans acquired at positions 1 and 2 indicated in (a); (d) IR spectra obtained at spots indicated in purple and gray, revealing two different chemical compositions where the purple one likely corresponds to smoother and lignin-rich domains.

The partially fragmented lignin (extracted, precipitated, and redeposited) on the surface of pretreated bagasse fibers may be more hydrophobic than anticipated due to the high temperatures at which it was processed (i.e., by following the normal foam preparation protocol). During the alkaline pretreatment, the temperature was set at 120 °C and cross-linking was performed at 150 °C. Gérardin and co-workers showed that the hydrophobicity of wood can be increased as a consequence of a thermal treatment at 130−160 °C, which is attributed to lignin conformational changes.[81] In addition, molecular dynamics simulations in water indicate that lignin conformational transitions are affected by both temperature and chain length.[78] When we produced a foam with fibers that had been subjected to an "extra" lignin precipitation step with a 120 °C thermal treatment, the foam was hydrophobic (Supporting Information, Figure S6). In this test, the dissolved lignin obtained from the liquid phase extracted during the alkaline pretreatment (0.8% lignin in 2% NaOH) was the lignin used in the precipitation step. On the other hand, foams with "extra" lignin, precipitated without heat treatment, were hydrophilic (data not shown since droplet is absorbed).

A recent example in the literature also describes a lignin coating used to improve surface hydrophobicity, but in contrast, the lignin is extracted in an acid medium with SO$_2$ followed by rinsing with water.[82] Comparing both methods, our alkaline extraction is more advantageous in terms of fiber hydrophobization because it does not involve the addition of functional groups to lignin, while the extraction with SO$_2$ leads to the addition of hydrophilic sulfates.[77] Furthermore, higher molecular weight fragments can be extracted with alkaline methods, which should be more hydrophobic.[83]

Finally, a test of oil absorption was carried out to analyze the ability of the foam to retain hydrophobic compounds (Figure 9). It was demonstrated that the foam was able to absorb an oil "spill" on the water surface, selectively extracting the oil from
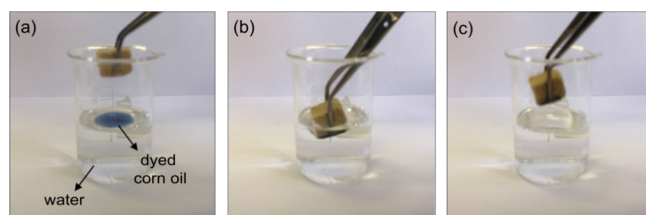
Figure 9. Selective removal of oil (stained with a blue dye, Sudan black B) from the water surface shown in panels (a) through (c): (a) oil spill on the water surface; (b) lignocellulosic foam absorbing oil (during 3 s); and (c) water surface without oil after absorption.

the water. The oil absorption capacity was the same for foams with and without chemical cross-linking, taking up approximately 9 g of oil per gram of lignocellulosic foam (ρ_{oil} = 0.92 g/cm^3). This performance is on the same order of magnitude as hydrophobic cellulose nanofibril (CNF) cryogels that can uptake 30 g of oil/g absorbent.[26] However, the preparation of hydrophobic CNF cryogels requires multiple (often costly) steps, including, for instance, styrene-acrylate grafting on the fibril surface, cross-linking with the polyamide-epichlorohydrin resin, and freeze-drying.[26] Similarly, sugarcane bagasse cryogels were recently introduced in the literature for oil spill cleanup, prepared by following two pretreatment steps (alkaline and bleaching), freeze-drying and curing with polyvinyl alcohol.[63] While the bagasse cryogels are capable of absorbing oil selectively, absorption capacity was not reported so we cannot compare directly to the work here. In contrast, our lignocellulosic foams from bagasse were obtained without the use of organic solvents or nonrenewable chemicals, using only two simple steps: (1) partial alkaline extraction of lignin, and (2) thermally-induced citric acid cross-linking and drying in a conventional oven.

CONCLUSIONS

Partial lignin extraction with dilute NaOH is the only pretreatment required to obtain highly hydrophobic lignocellulosic foams from sugarcane bagasse. These lightweight materials can be easily prepared by oven-drying aqueous dispersions of pretreated fibers. When dried in the presence of citric acid, the network becomes cross-linked and wet-stable. This method represents a new approach to hydrophobic materials derived from plant biomass, which follows some of the principles of green chemistry,[84] namely, (3) *less hazardous chemical synthesis*, since the preparation does not require any synthetic chemical additives to produce hydrophobic materials; (5) *safer solvents and auxiliaries*, as the route is water-based and free of organic solvents and the cross-linker is citric acid, which is food-safe; (6) *design for energy efficiency*, because the foams were oven-dried (after straightforward dewatering), without the need for vacuum or pressure conditions; (7) *use of renewable feedstocks*, using sugarcane bagasse as the lignocellulosic source; and (10) *design for degradation*, since the lignocellulosic foams obtained in this work are fully bio-based, biodegradable, and safe for the environment.

The lignocellulosic foams developed here can be compressed in oil and water without disintegrating and are able to store and release mechanical energy as a result of their elastic shape-recovery properties. They are naturally hydrophobic (θ = 117°) due to the combination of surface lignin and surface structure/roughness, from the high pH and temperature conditions employed during pretreatment, and the rough air-trapped foam network. Mechanical resistance in water along with selective oil absorption abilities suggests that these lignocellulosic foams are suitable for applications involving extractions at water/oil interfaces, such as oil spills and effluent treatment or as replacements for more conventional protective, insulating, and sorption materials typically made from inorganic compounds or synthetic polymers.

ASSOCIATED CONTENT

ⓈI Supporting Information

The Supporting Information is available free of charge at https://pubs.acs.org/doi/10.1021/acssuschemeng.0c01480.

> Compositional information of sugarcane bagasse samples; basis weight and density of foams and other lightweight fiber materials; cross-section of cross-linked foams by FESEM; reconstructed view of a cross-linked foam by micro-CT analysis; elemental composition of bagasse samples by XPS; surface roughness profile by micro-CT analysis; and photographs of wettability and lignin precipitation tests (PDF)

> Micro-CT video showing the foam structure (MP4)

AUTHOR INFORMATION

Corresponding Authors

Emily D. Cranston − *Department of Chemical Engineering, McMaster University, Hamilton, Ontario L8S 4L7, Canada; Department of Wood Science and Department of Chemical and Biological Engineering, University of British Columbia, Vancouver, British Columbia V6T 1Z4, Canada;* ⓄRCID orcid.org/0000-0003-4210-9787; Email: emily.cranston@ubc.ca

Camila A. Rezende − *Institute of Chemistry, University of Campinas, Campinas, São Paulo 13083-970, Brazil;* Ⓞ orcid.org/0000-0002-2072-1361; Email: camilaiq@unicamp.br

Author

Elisa S. Ferreira − *Institute of Chemistry, University of Campinas, Campinas, São Paulo 13083-970, Brazil; Department of Chemical Engineering, McMaster University, Hamilton, Ontario L8S 4L7, Canada;* Ⓞ orcid.org/0000-0002-3614-5012

Complete contact information is available at:
https://pubs.acs.org/10.1021/acssuschemeng.0c01480

Notes

The authors declare no competing financial interest.

■ REFERENCES

(1) Alimadadi, M.; Uesaka, T. 3D-Oriented Fiber Networks Made by Foam Forming. *Cellulose* **2016**, *23*, 661−671.

(2) Nechita, P.; Năstac, S. Foam-Formed Cellulose Composite Materials with Potential Applications in Sound Insulation. *J. Compos. Mater.* **2017**, *52*, 747−754.

(3) Ferreira, E. S.; Rezende, C. A. Simple Preparation of Cellulosic Lightweight Materials from Eucalyptus Pulp. *ACS Sustainable Chem. Eng.* **2018**, *6*, 14365−14373.

(4) Timofeev, O.; Jetsu, P.; Kiiskinen, H.; Keränen, J. T. Drying of Foam-Formed Mats from Virgin Pine Fibers. *Drying Technol.* **2016**, *34*, 1210−1218.

(5) Chen, W.; Yu, H.; Li, Q.; Liu, Y.; Li, J. Ultralight and Highly Flexible Aerogels with Long Cellulose I Nanofibers. *Soft Matter* **2011**, *7*, 10360−10368.

(6) De France, K. J.; Hoare, T.; Cranston, E. D. Review of Hydrogels and Aerogels Containing Nanocellulose. *Chem. Mater.* **2017**, *29*, 4609−4631.

(7) Lavoine, N.; Bergström, L. Nanocellulose-Based Foams and Aerogels: Processing, Properties, and Applications. *J. Mater. Chem. A* **2017**, *5*, 16105−16117.

(8) Zhao, S.; Malfait, W. J.; Guerrero-Alburquerque, N.; Koebel, M. M.; Nyström, G. Biopolymer Aerogels and Foams: Chemistry, Properties, and Applications. *Angew. Chem. Int. Ed.* **2018**, *57*, 7580−7608.

(9) Pöhler, T.; Jetsu, P.; Isomoisio, H. Benchmarking New Wood Fibre−Based Sound Absorbing Material Made with a Foam-Forming Technique. *Build. Acoust.* **2016**, *23*, 131−143.

(10) Madani, A.; Zeinoddini, S.; Varahmi, S.; Turnbull, H.; Phillion, A. B.; Olson, J. A.; Martinez, D. M. Ultra-Lightweight Paper Foams: Processing and Properties. *Cellulose* **2014**, *21*, 2023−2031.

(11) Burke, S. R.; Möbius, M. E.; Hjelt, T.; Hutzler, S. Properties of Lightweight Fibrous Structures Made by a Novel Foam Forming Technique. *Cellulose* **2019**, *26*, 2529−2539.

(12) Janko, M.; Jocher, M.; Boehm, A.; Babel, L.; Bump, S.; Biesalski, M.; Meckel, T.; Stark, R. W. Cross-Linking Cellulosic Fibers with Photoreactive Polymers: Visualization with Confocal Raman and Fluorescence Microscopy. *Biomacromolecules* **2015**, *16*, 2179−2187.

(13) Lindström, T.; Wågberg, L.; Larsson, T. On the Nature of Joint Strength in Paper − A Review of Dry and Wet Strength Resins Used in Paper Manufacturing. In *Proc. 13th Fundamental Research Symp*; Cambridge, 2005.

(14) Liang, L.; Bhagia, S.; Li, M.; Huang, C.; Ragauskas, A. J. Cross-Linked Nanocellulosic Materials and Their Applications. *ChemSusChem* **2019**, *13*, 78.

(15) Demitri, C.; del Sole, R.; Scalera, F.; Sannino, A.; Vasapollo, G.; Maffezzoli, A.; Ambrosio, L.; Nicolais, L. Novel Superabsorbent Cellulose-Based Hydrogels Crosslinked with Citric Acid. *J. Appl. Polym. Sci.* **2008**, *110*, 2453−2460.

(16) Toledo, P. V. O.; Limeira, D. P. C.; Siqueira, N. C.; Petri, D. F. S. Carboxymethyl Cellulose/Poly(Acrylic Acid) Interpenetrating Polymer Network Hydrogels as Multifunctional Adsorbents. *Cellulose* **2019**, *26*, 597−615.

(17) Toledo, P. V. O.; Martins, B. F.; Pirich, C. L.; Sierakowski, M. R.; Neto, E. T.; Petri, D. F. S. Cellulose Based Cryogels as Adsorbents for Organic Pollutants. *Macromol. Symp.* **2019**, *383*, 1800013.

(18) Meftahi, A.; Khajavi, R.; Rashidi, A.; Rahimi, M. K.; Bahador, A. Preventing the Collapse of 3D Bacterial Cellulose Network via Citric Acid. *J. Nanostruct. Chem.* **2018**, *8*, 311−320.

(19) Ottenhall, A.; Seppänen, T.; Ek, M. Water-Stable Cellulose Fiber Foam with Antimicrobial Properties for Bio Based Low-Density Materials. *Cellulose* **2018**, *25*, 2599−2613.

(20) Belosinschi, D.; Tofanica, B.-M. A New Bio-Material with 3D Lightweight Network for Energy and Advanced Applications. *Cellulose* **2018**, *25*, 897−902.

(21) Klemm, D.; Philipp, B.; Heinze, T.; Heinze, U.; Wagenknecht, W. *Comprehensive Cellulose Chemistry*; Wiley-VCH Verlag GmbH & Co. KGaA, 1998.

(22) Medronho, B.; Romano, A.; Miguel, M. G.; Stigsson, L.; Lindman, B. Rationalizing Cellulose (in)Solubility: Reviewing Basic Physicochemical Aspects and Role of Hydrophobic Interactions. *Cellulose* **2012**, *19*, 581−587.

(23) Hubbe, M. A.; Gardner, D. J.; Shen, W. Contact Angles and Wettability of Cellulosic Surfaces: A Review of Proposed Mechanisms and Test Strategies. *BioResources* **2015**, *10*, 8657−8749.

(24) Chin, S. F.; Binti Romainor, A. N.; Pang, S. C. Fabrication of Hydrophobic and Magnetic Cellulose Aerogel with High Oil Absorption Capacity. *Mater. Lett.* **2014**, *115*, 241−243.

(25) Laitinen, O.; Suopajärvi, T.; Österberg, M.; Liimatainen, H. Hydrophobic, Superabsorbing Aerogels from Choline Chloride-Based Deep Eutectic Solvent Pretreated and Silylated Cellulose Nanofibrils for Selective Oil Removal. *ACS Appl. Mater. Interfaces* **2017**, *9*, 25029−25037.

(26) Mulyadi, A.; Zhang, Z.; Deng, Y. Fluorine-Free Oil Absorbents Made from Cellulose Nanofibril Aerogels. *ACS Appl. Mater. Interfaces* **2016**, *8*, 2732−2740.

(27) Fumagalli, M.; Ouhab, D.; Boisseau, S. M.; Heux, L. Versatile Gas-Phase Reactions for Surface to Bulk Esterification of Cellulose Microfibrils Aerogels. *Biomacromolecules* **2013**, *14*, 3246−3255.

(28) Lin, N.; Huang, J.; Chang, P. R.; Feng, J.; Yu, J. Surface Acetylation of Cellulose Nanocrystal and Its Reinforcing Function in Poly(Lactic Acid). *Carbohydr. Polym.* **2011**, *83*, 1834−1842.

(29) Österberg, M.; Vartiainen, J.; Lucenius, J.; Hippi, U.; Seppälä, J.; Serimaa, R.; Laine, J. A Fast Method to Produce Strong NFC Films as a Platform for Barrier and Functional Materials. *ACS Appl. Mater. Interfaces* **2013**, *5*, 4640−4647.

(30) Hu, Z.; Berry, R. M.; Pelton, R.; Cranston, E. D. One-Pot Water-Based Hydrophobic Surface Modification of Cellulose Nanocrystals Using Plant Polyphenols. *ACS Sustainable Chem. Eng.* **2017**, *5*, 5018−5026.

(31) Habibi, Y. Key Advances in the Chemical Modification of Nanocelluloses. *Chem. Soc. Rev.* **2014**, *43*, 1519−1542.

(32) Eriksson, T.; Börjesson, J.; Tjerneld, F. Mechanism of Surfactant Effect in Enzymatic Hydrolysis of Lignocellulose. *Enzyme Microb. Technol.* **2002**, *31*, 353−364.

(33) Heiss-Blanquet, S.; Zheng, D.; Ferreira, N. L.; Lapierre, C.; Baumberger, S. Effect of Pretreatment and Enzymatic Hydrolysis of Wheat Straw on Cell Wall Composition, Hydrophobicity and Cellulase Adsorption. *Bioresour. Technol.* **2011**, *102*, 5938−5946.

(34) Rojo, E.; Peresin, M. S.; Sampson, W. W.; Hoeger, I. C.; Vartiainen, J.; Laine, J.; Rojas, O. J. Comprehensive Elucidation of the Effect of Residual Lignin on the Physical, Barrier, Mechanical and Surface Properties of Nanocellulose Films. *Green Chem.* **2015**, *17*, 1853−1866.

(35) Imani, M.; Ghasemian, A.; Dehghani-Firouzabadi, M. R.; Afra, E.; Gane, P. A. C.; Rojas, O. J. Nano-Lignocellulose from Recycled Fibres in Coatings from Aqueous and Ethanolic Media: Effect of Residual Lignin on Wetting and Offset Printing Quality. *Nord. Pulp Pap. Res. J.* **2019**, *34*, 200−210.

(36) Nelson, K.; Retsina, T. Innovative Nanocellulose Process Breaks the Cost Barrier. *Tappi J.* **2014**, *13*, 19−23.

(37) Zhang, L.; Lu, H.; Yu, J.; Fan, Y.; Ma, J.; Wang, Z. Contribution of Lignin to the Microstructure and Physical Performance of Three-Dimensional Lignocellulose Hydrogels. *Cellulose* **2019**, *26*, 2375−2388.

(38) Bassam, N. E. *Handbook of Bioenergy Crops: A Complete Reference to Species, Development and Applications*, 1st ed.; Earthscan: Oxon, 2010.

(39) Loh, Y. R.; Sujan, D.; Rahman, M. E.; Das, C. A. Sugarcane Bagasse—The Future Composite Material: A Literature Review. *Resour. Conserv. Recycl.* **2013**, *75*, 14−22.

(40) Chandel, A. K.; da Silva, S. S.; Carvalho, W.; Singh, O. V. Sugarcane Bagasse and Leaves: Foreseeable Biomass of Biofuel and Bio-Products. *J. Chem. Technol. Biotechnol.* **2012**, *87*, 11−20.

(41) Rezende, C.; de Lima, M.; Maziero, P.; deAzevedo, E.; Garcia, W.; Polikarpov, I. Chemical and Morphological Characterization of

Sugarcane Bagasse Submitted to a Delignification Process for Enhanced Enzymatic Digestibility. *Biotechnol. Biofuels* **2011**, *4*, 54.

(42) Rattanaporn, K.; Tantayotai, P.; Phusantisampan, T.; Pornwongthong, P.; Sriariyanun, M. Organic Acid Pretreatment of Oil Palm Trunk: Effect on Enzymatic Saccharification and Ethanol Production. *Bioprocess Biosyst. Eng.* **2018**, *41*, 467–477.

(43) Moreira-Vilar, F. C.; Siqueira-Soares, R. D. C.; Finger-Teixeira, A.; de Oliveira, D. M.; Ferro, A. P.; da Rocha, G. J.; Ferrarese, M. D. L. L.; dos Santos, W. D.; Ferrarese-Filho, O. The Acetyl Bromide Method Is Faster, Simpler and Presents Best Recovery of Lignin in Different Herbaceous Tissues than Klason and Thioglycolic Acid Methods. *PLoS One* **2014**, *9*, e110000.

(44) Stamm, A. J. Density of Wood Substance, Adsorption by Wood, and Permeability of Wood. *J. Phys. Chem.* **1929**, *33*, 398–414.

(45) Ehrnrooth, E. M. L. Change in Pulp Fibre Density With Acid-Chlorite Delignification. *J. Wood Chem. Technol.* **2006**, *4*, 91–109.

(46) Mello, L. R.; Hamley, I. W.; Miranda, A.; Alves, W. A.; Silva, E. R. β-Sheet Assembly in Amyloidogenic Glutamic Acid Nanostructures: Insights from X-Ray Scattering and Infrared Nanospectroscopy. *J. Pept. Sci.* **2019**, *25*, No. e3170.

(47) Driemeier, C.; Oliveira, M. M.; Mendes, F. M.; Gómez, E. O. Characterization of Sugarcane Bagasse Powders. *Powder Technol.* **2011**, *214*, 111–116.

(48) Schutyser, W.; Renders, T.; van den Bosch, S.; Koelewijn, S.-F.; Beckham, G. T.; Sels, B. F. Chemicals from Lignin: An Interplay of Lignocellulose Fractionation, Depolymerisation, and Upgrading. *Chem. Soc. Rev.* **2018**, *47*, 852–908.

(49) Latarullo, M. B. G.; Tavares, E. Q. P.; Padilla, G.; Leite, D. C. C.; Buckeridge, M. S. Pectins, Endopolygalacturonases, and Bioenergy. *Front. Plant Sci.* **2016**, *7*, 1401.

(50) Brandt, A.; Gräsvik, J.; Hallett, J. P.; Welton, T. Deconstruction of Lignocellulosic Biomass with Ionic Liquids. *Green Chem.* **2013**, *15*, 550–583.

(51) Lima, M. A.; Lavorente, G. B.; da Silva, H. K.; Bragatto, J.; Rezende, C. A.; Bernardinelli, O. D.; deAzevedo, E. R.; Gomez, L. D.; Mcqueen-Mason, S. J.; Labate, C. A.; Polikarpov, I. Effects of Pretreatment on Morphology, Chemical Composition and Enzymatic Digestibility of Eucalyptus Bark: A Potentially Valuable Source of Fermentable Sugars for Biofuel Production — Part 1. *Biotechnol. Biofuels* **2013**, *6*, 75.

(52) Zhu, Z.; Rezende, C. A.; Simister, R.; McQueen-Mason, S. J.; Macquarrie, D. J.; Polikarpov, I.; Gomez, L. D. Efficient Sugar Production from Sugarcane Bagasse by Microwave Assisted Acid and Alkali Pretreatment. *Biomass Bioenergy* **2016**, *93*, 269–278.

(53) Hirn, U.; Bauer, W. A Review of Image Analysis Based Methods to Evaluate Fiber Properties. *Lenzing. Berichte* **2006**, *86*, 96–105.

(54) Agnihotri, S.; Dutt, D.; Tyagi, C. H. Complete Characterization of Bagasse of Early Specie of Saccharum Officinerum-Co 89003 for Pulp and Paper Making. *BioResources* **2010**, *5*, 1197–1214.

(55) Li, B.; Bandekar, R.; Zha, Q.; Alsaggaf, A.; Ni, Y. Fiber Quality Analysis: OpTest Fiber Quality Analyzer versus L&W Fiber Tester. *Ind. Eng. Chem. Res.* **2011**, *50*, 12572–12578.

(56) Liu, J.; Liu, Q.; Ma, D.; Yuan, Y.; Yao, J.; Zhang, W.; Su, H.; Su, Y.; Gu, J.; Zhang, D. Simultaneously Achieving Thermal Insulation and Rapid Water Transport in Sugarcane Stems for Efficient Solar Steam Generation. *J. Mater. Chem. A* **2019**, *7*, 9034–9039.

(57) de Souza, A. P.; Leite, D. C. C.; Pattathil, S.; Hahn, M. G.; Buckeridge, M. S. Composition and Structure of Sugarcane Cell Wall Polysaccharides: Implications for Second-Generation Bioethanol Production. *BioEnergy Res.* **2013**, *6*, 564–579.

(58) He, L.; Terashima, N. Formation and Structure of Lignin in Monocotyledons IV. Deposition Process and Structural Diversity of the Lignin in the CellWall of Sugarcane and Rice Plant Studied by Ultraviolet Microscopic Spectroscopy. *Holzforschung* **1991**, *45*, 191–198.

(59) Waterhouse, J. F. Paper Products: Classification. In *Encyclopedia of Materials: Science and Technology*; Buschow, K. H. J., Cahn, R. W., Flemings, M. C., Ilschner, B., Kramer, E. J., Mahajan, S., Veyssière, P., Eds.; Elsevier: Oxford, 2001; pp 6685–6696, DOI: DOI: 10.1016/B0-08-043152-6/01183-9.

(60) *TAPPI T 441: Water Absorptiveness of Sized (Non-Bibulous) Paper, Paperboard, and Corrugated Fiberboard (Cobb Test)*. TAPPI 1998.

(61) Yancy-Caballero, D.; Ling, L. Y.; Archilha, N. L.; Ferreira, J. E.; Driemeier, C. Mineral Particles in Sugar Cane Bagasse: Localization and Morphometry Using Microtomography Analysis. *Energy Fuels* **2017**, *31*, 12288–12296.

(62) Ashby, M. F.; Medalist, R. F. M. The Mechanical Properties of Cellular Solids. *Metall. Trans. A* **1983**, *14*, 1755–1769.

(63) Thai, Q. B.; Nguyen, S. T.; Ho, D. K.; Tran, T. D.; Huynh, D. M.; Do, N. H. N.; Luu, T. P.; Le, P. K.; Le, D. K.; Phan-Thien, N.; Duong, H. M. Cellulose-Based Aerogels from Sugarcane Bagasse for Oil Spill-Cleaning and Heat Insulation Applications. *Carbohydr. Polym.* **2020**, *228*, 115365.

(64) Ferreira, E. S.; Lanzoni, E. M.; Costa, C. A. R.; Deneke, C.; Bernardes, J. S.; Galembeck, F. Adhesive and Reinforcing Properties of Soluble Cellulose: A Repulpable Adhesive for Wet and Dry Cellulosic Substrates. *ACS Appl. Mater. Interfaces* **2015**, *7*, 18750–18758.

(65) Roberts, J. C. *The Chemistry of Paper*; Royal Society of Chemistry: Cambridge, 1996.

(66) Persson, B. N. J.; Ganser, C.; Schmied, F.; Teichert, C.; Schennach, R.; Gilli, E.; Hirn, U. Adhesion of Cellulose Fibers in Paper. *J. Phys. Condens. Matter* **2013**, *25*, No. 045002.

(67) Hirn, U.; Schennach, R. Comprehensive Analysis of Individual Pulp Fiber Bonds Quantifies the Mechanisms of Fiber Bonding in Paper. *Sci. Rep.* **2015**, *5*, 10503.

(68) Mark, R. E. *Handbook of Physical and Mechanical Testing of Paper and Paperboard*; Dekker, 1983; Vol. *1*.

(69) Espy, H. H. The Mechanism of Wet-Strength Development in Paper: A Review. *Tappi J.* **1995**, *78*, 90.

(70) Gustafsson, E.; Wang, Z.; Polat, O.; Ostendorf, W. W.; Sheehan, J. G.; Pelton, R. Towards Wet Resilient Paper — Fiber Modifications and Test Method. In *Advances in Pulp and Paper Research*; FRC: Oxford, 2017; pp 865–894.

(71) Parmenter, K. E.; Milstein, F. Mechanical Properties of Silica Aerogels. *J. Non-Cryst. Solids* **1998**, *223*, 179–189.

(72) Mbiada, A. A. Y.; Musa, S.; Richter, O.; Kneer, A.; Barbe, S. Controlling Surface Hydrophobicity of Cellulose-Lignin Composite Coatings. *Polym. Renew. Res.* **2018**, *9*, 51–58.

(73) Gu, L.; Jiang, B.; Song, J.; Jin, Y.; Xiao, H. Effect of Lignin on Performance of Lignocellulose Nanofibrils for Durable Super-hydrophobic Surface. *Cellulose* **2019**, *26*, 933–944.

(74) Zeng, Y.; Zhao, S.; Yang, S.; Ding, S.-Y. Lignin Plays a Negative Role in the Biochemical Process for Producing Lignocellulosic Biofuels. *Curr. Opin. Biotechnol.* **2014**, *27*, 38–45.

(75) Lievonen, M.; Valle-Delgado, J. J.; Mattinen, M.-L.; Hult, E.-L.; Lintinen, K.; Kostiainen, M. A.; Paananen, A.; Szilvay, G. R.; Setälä, H.; Österberg, M. A Simple Process for Lignin Nanoparticle Preparation. *Green Chem.* **2016**, *18*, 1416–1422.

(76) Trevisan, H.; Rezende, C. A. Pure, Stable and Highly Antioxidant Lignin Nanoparticles from Elephant Grass. *Ind. Crop. Prod.* **2020**, *145*, 112105.

(77) Kai, D.; Tan, M. J.; Chee, P. L.; Chua, Y. K.; Yap, Y. L.; Loh, X. J. Towards Lignin-Based Functional Materials in a Sustainable World. *Green Chem.* **2016**, *18*, 1175–1200.

(78) Petridis, L.; Smith, J. C. Conformations of Low-Molecular-Weight Lignin Polymers in Water. *ChemSusChem* **2016**, *9*, 289–295.

(79) Quéré, D. Wetting and Roughness. *Annu. Rev. Mater. Res.* **2008**, *38*, 71–99.

(80) Dorrer, C.; Rühe, J. Some Thoughts on Superhydrophobic Wetting. *Soft Matter* **2009**, *5*, 51–61.

(81) Hakkou, M.; Pétrissans, M.; Zoulalian, A.; Gérardin, P. Investigation of Wood Wettability Changes during Heat Treatment on the Basis of Chemical Analysis. *Polym. Degrad. Stab.* **2005**, *89*, 1–5.

(82) Nelson, K.; Retsina, T.; Pylkkanen, V.; O'Connor, R. Processes for Producing Lignin-Coated Hydrophobic Cellulose, and Compositions and Products Produced Therefrom. US20150232703A1, August 20, 2015.

(83) Nitsos, C.; Stoklosa, R.; Karnaouri, A.; Vörös, D.; Lange, H.; Hodge, D.; Crestini, C.; Rova, U.; Christakopoulos, P. Isolation and Characterization of Organosolv and Alkaline Lignins from Hardwood and Softwood Biomass. *ACS Sustainable Chem. Eng.* **2016**, *4*, 5181−5193.

(84) 12 Principles of Green Chemistry   https://www.acs.org/content/acs/en/greenchemistry/principles/12-principles-of-green-chemistry.html (accessed Feb 20, 2020).